Mechanism(s) of action of heavy metals to investigate the regulation of plastidic glucose-6-phosphate dehydrogenase

Alessia DE LILLO, Manuela CARDI, Simone LANDI, Sergio ESPOSITO*

* sergio.esposito@unina.it

Supplementary Information

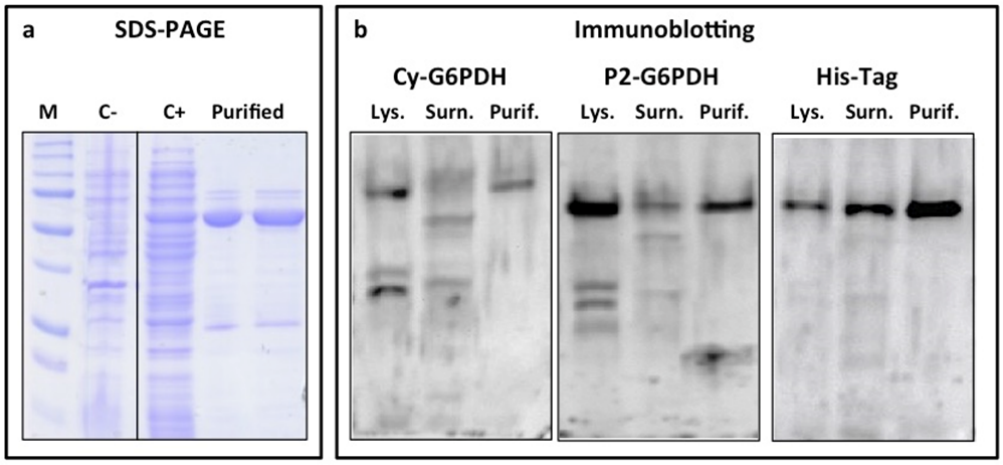

Supplementary Figure S1. Electrophoretic analysis and immunoblots of *Pt*P2-G6PDH WT.

(a) Coomassie-stained SDS gels showing a protein of the expected MW corresponding to *Pt*P2-G6PDH WT. M, Markers; C-, Control (*E. coli* without transformed plasmid); C+, transformed colonies after induction with IPTG; Purified, purified protein after IMAC step, 5µg and 10 µg protein.

(b) Immunoblotting using antisera versus Cy-G6PDH antiserum (potato[14]); P2-G6PDH antiserum (potato[14]); His_6-tag antiserum (Roche). Legend for the lanes: Lys., bacterial lysate; Surn., surnatant or soluble fraction; Purif., purified protein as in (a).

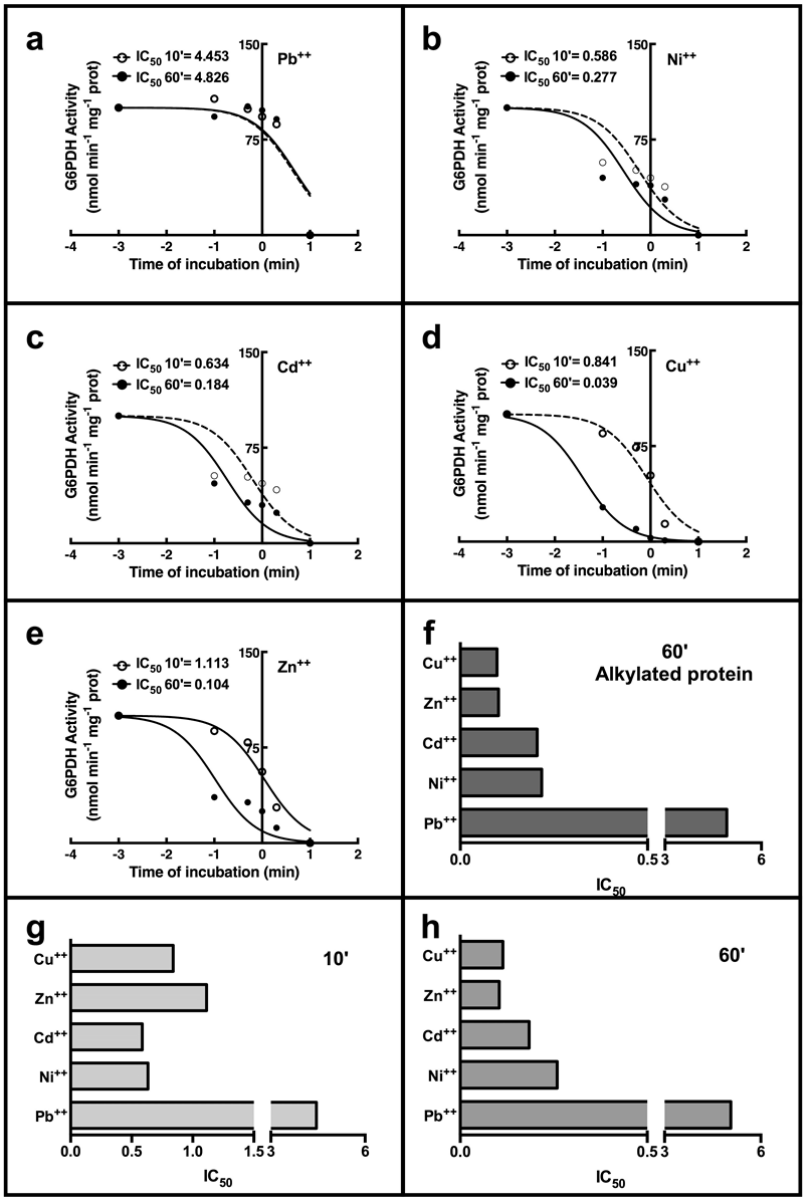

Supplementary Figure S2. Determination of IC_{50} values (mM) calculated after 10' (open circles, dotted line) and 60' (close circles, solid line) of incubation with different HMs related to *Pt*P2-G6PDH WT activity. (a) Pb^{++}; (b) Ni^{++}; (c) Cd^{++}; (d) Cu^{++}; (e) Zn^{++}; (f) IC_{50} values (mM) after 60' of incubation with each metal, as calculated on alkylated enzyme to assess the influence of his-tag on HM binding; (g) and (h), IC_{50} values (mM) for each metal as calculated from the graphs (a) to (e) on his-tagged *Pt*P2-G6PDH, after 10' and 60' of incubation, respectively. R^2 for IC50 was between 70 and 98% (not shown). Non-linear regressions and IC_{50} values were calculated by Graph-Pad Prism software.

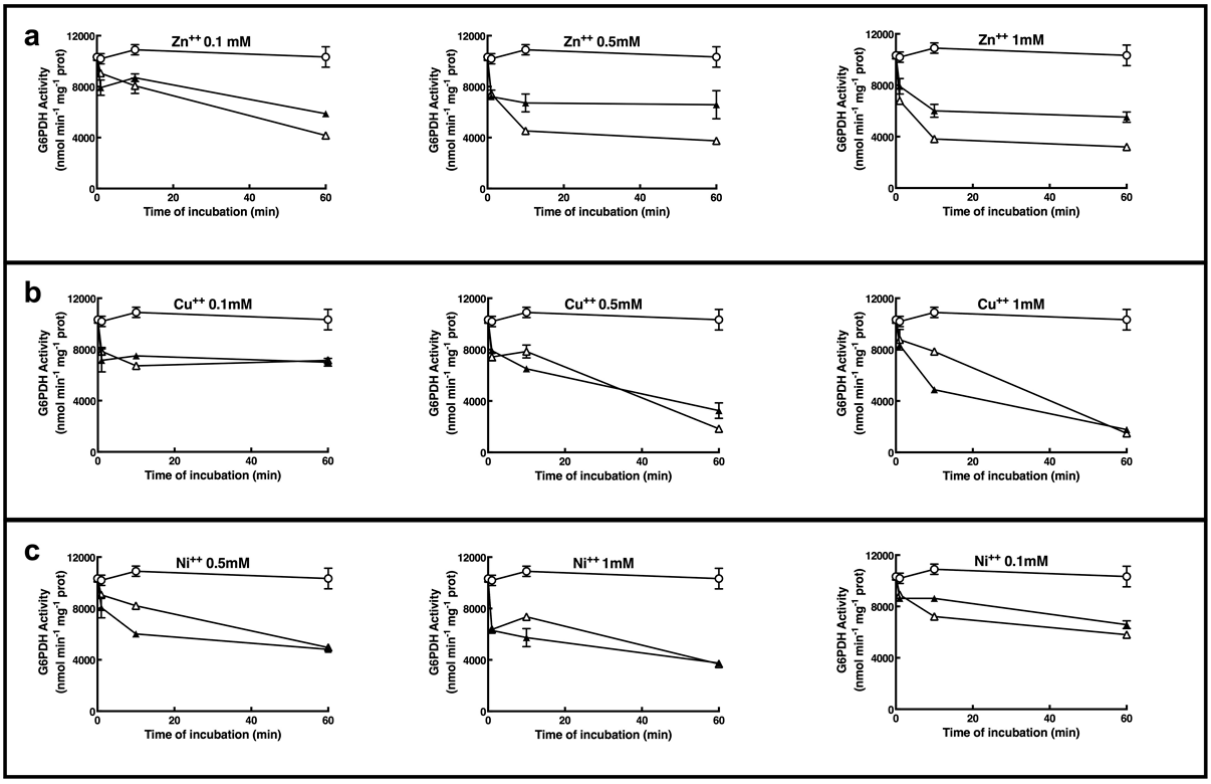

Supplementary Figure S3. Comparison between the effects of chloride and sulphate salts of heavy metals on recombinant *Pt*P2-G6PDH WT activity.

Purified enzyme was incubated without heavy metals (○); or in the presence of different metals chloride (▲) and sulfate (△) salts at increasing concentrations: 0.1mM (left); 0.5mM (center), 1mM (right) for 1, 10, 60 min. (a) Zinc (Zn^{++}); (b) Copper (Cu^{++}); (c) Nickel (Ni^{++}).

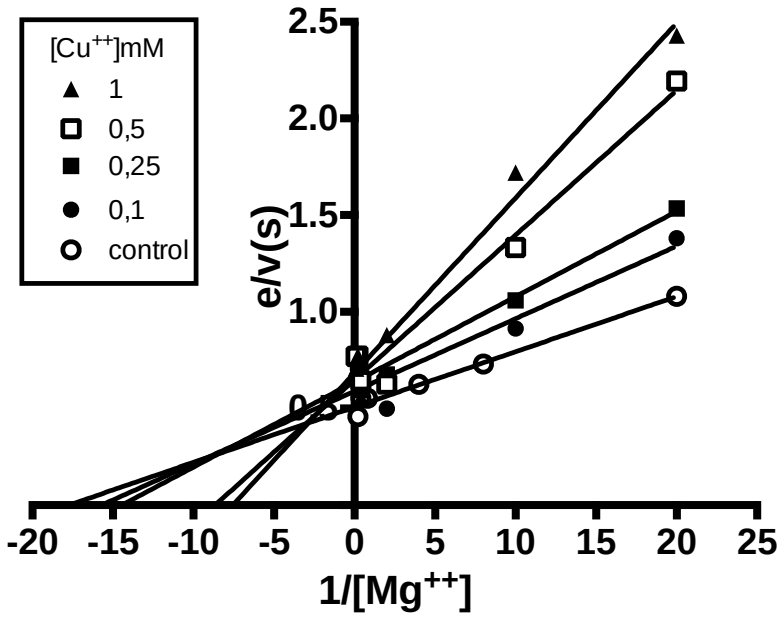

Supplementary Figure S4. Double reciprocal plot of competition experiment measuring Km_{Mg}^{++} in the presence of increasing levels of Cu^{++} on *Pt*P2-G6PDH.

Purified enzyme was desalted on Sephadex G25 twice to obtain a no-Mg^{++} enzyme. Then this preparation was tested to determine Km_{Mg}^{++}= 0.060 mM (V_{max}: 1.9 mM). When desalted (no-Mg^{++}) enzyme was exposed to Cu^{++} levels from 0 to 1mM (as indicated in the in-figure legend), Kms_{Mg}^{++} increased up to 0.15mM; V_{max} remained substantially unchanged, 1.68 ± 0.16mM.

Copper was provided as $CuCl_2$ to avoid possible sulphate inhibition.

The regressions were calculated by Graphpad Prism software within 91-98% confidence.

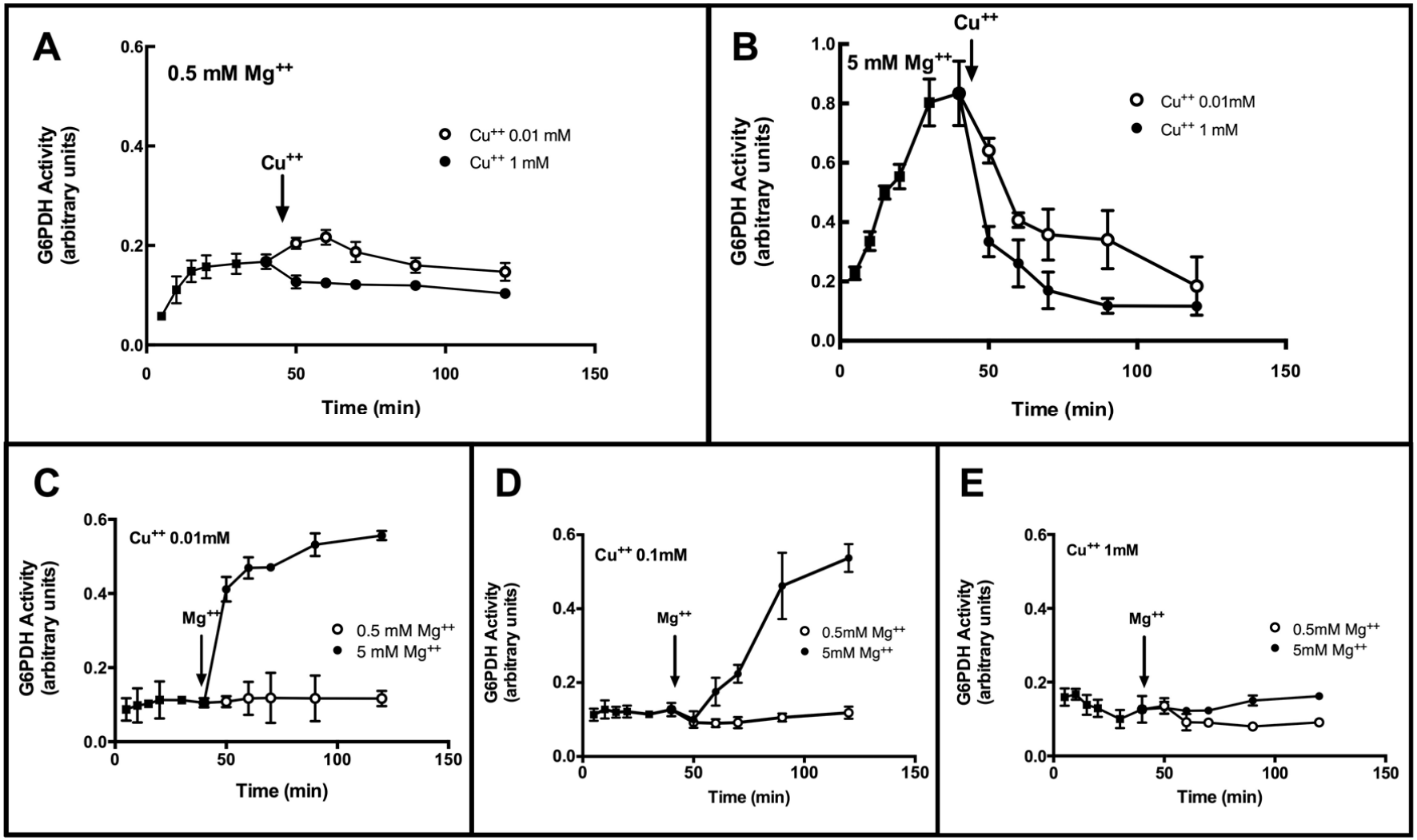
A
0.5 mM Mg++
Cu++
Cu++ 0.01 mM
Cu++ 1 mM
G6PDH Activity (arbitrary units)
Time (min)
B
5 mM Mg++
Cu++
Cu++ 0.01mM
Cu++ 1 mM
G6PDH Activity (arbitrary units)
Time (min)
C
Cu++ 0.01mM
Mg++
0.5 mM Mg++
5 mM Mg++
G6PDH Activity (arbitrary units)
Time (min)
D
Cu++ 0.1mM
Mg++
0.5mM Mg++
5mM Mg++
G6PDH Activity (arbitrary units)
Time (min)
E
Cu++ 1mM
Mg++
0.5mM Mg++
5mM Mg++
G6PDH Activity (arbitrary units)
Time (min)

Supplementary Figure S5. Tests for reversibility of Cu^{++} inhibition of *Pt*P2-G6PDH activity. Purified enzyme was desalted on Sephadex G25 twice to obtain an enzyme containing no Mg^{++}. Then, this preparation was tested for G6PDH activity in assay mixture in the presence of 0.5mM Mg^{++} (A); or 5mM Mg^{++} (B). After 45min, when enzyme activity was stable, 0.01mM or 1mM Cu^{++} were added to the assay mix and the inhibition of the activity measured.

In the second set of measurements, the enzyme containing no Mg^{++} was tested for G6PDH activity in assay mixture in the presence of 0.01mM (C); 0.1mM (D), and 1mM (E) Cu^{++} after 45min, when enzyme activity was stable, 0.5mM Mg^{++} or 5mM Mg^{++} were added to the assay mix and the re-activation of activity measured.

Copper was provided as $CuCl_2$ to avoid possible sulphate inhibition. The error bars indicate standard error from at least three different measurements.

	Km_{G6P} (mM)	Km_{NADP^+} (µM)	Ki_{NADPH} (µM)	V_{max} ($U \cdot mg^{-1}$ prot)	Monomer MW His-tagged (kDa)
*Pt*P2-G6PDH WT	0.95± 0.12	28 ± 4	73 ± .3	7800	**64**
*Pt*P2-G6PDH WT*	1.06 ± 0.06	15 ± 3	74.1 ± 2.5	8000	**61**

Supplementary Table S1 - Kinetic properties of wild type recombinant G6PDH from *Populus trichocarpa* (*Pt*P2-G6PDH WT). In the first line, the main kinetic properties measured in purified protein preparations used in this study; in the second line the previously published parameters for the same enzyme[22]. Molecular weights were calculated by using the relative mobility factor method in SDS-PAGE (gels and immunoblotting are shown in Supplementary Figure S1).

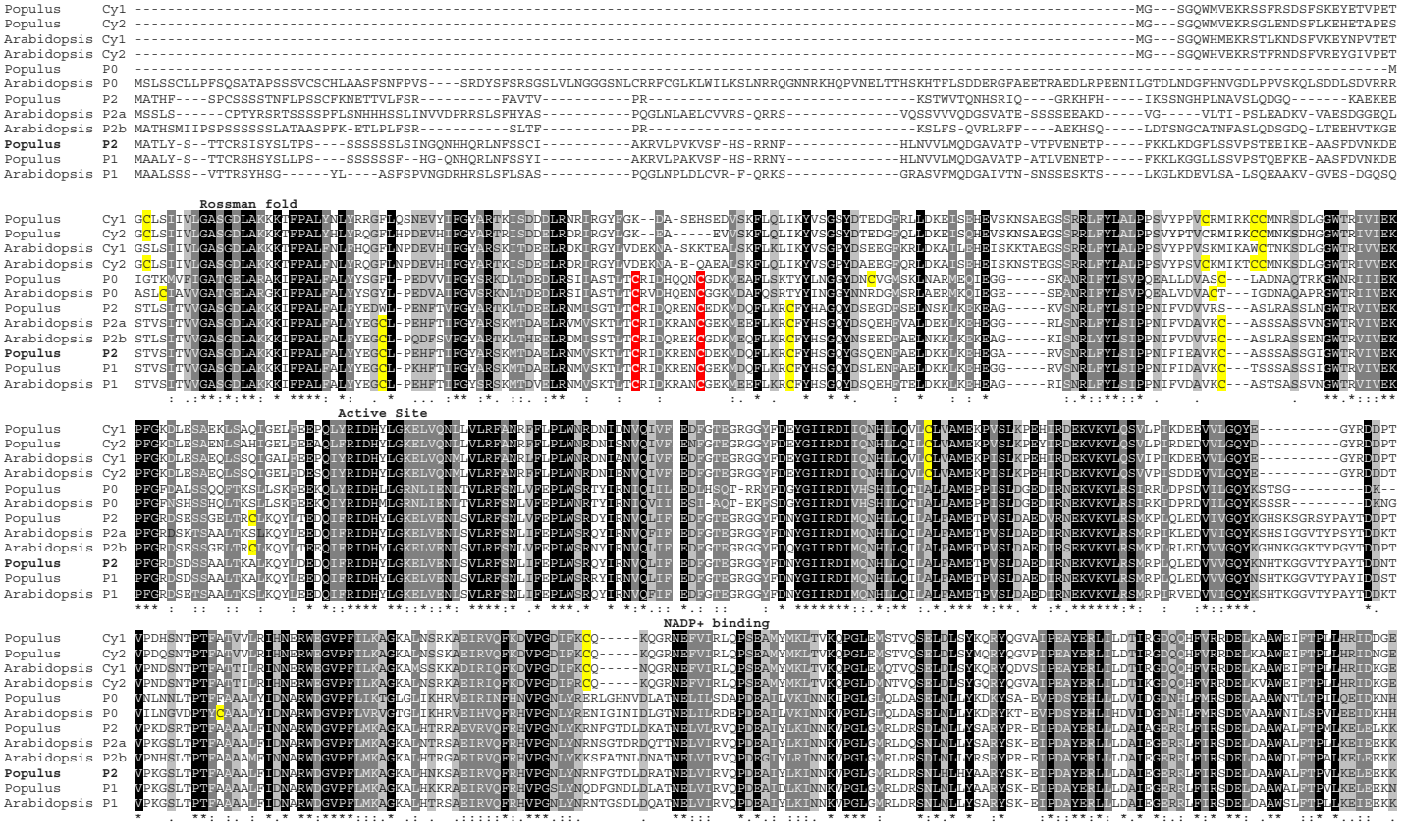
Rossman fold
Active Site
NADP+ binding

Supplementary Table S2. Comparison among aminoacidic sequences of G6PDH isoforms from *Populus* and *Arabidopsis*. Legend: CY, cytosolic isoform; P0, peroxisome/cytosolic/plastidial isoform; P1, chloroplastic isoform; P2, plastidial isoform. Typical motifs are indicated: Rossman-fold; active site, and $NADP^+$ binding site. Cysteine residues present in the sequences are highlighted in yellow. Regulatory cysteines involved in the formation of the disulfide are in white letters highlighted in red. Conservation of residues in the different sequences is indicated in grey scale from white (no conservation) to black (same residue in all isoforms).

List of sequences: *Populus* CYa, estExt_Genewise1_v1.C_LG_XVII0625; *Populus* CYb, grail3.0054015801; *Arabidopsis* CYa At3g27300.1; *Arabidopsis* CYb At5g40760.1; *Populus* P0, estExt_fgenesh4_pm.C_LG_XIII0018; *Arabidopsis* P0, At1g09420.1; *Populus* P1, fgenesh4_pm.C_LG_XIV000487; *Arabidopsis* P1, At5g13110.1; *Arabidopsis* P2a, At1g24280.1; *Arabidopsis* P2b, At5g35790.1; *Populus* P2a, estExt_Genewise1_v1.C_LG_I7789; *Populus* P2b, eugene3.0003137

Supplementary Table S3. Report of theoretical models utilised in this work for putative 3D modelling of *Pt*P2-G6PDH WT.

*Pt*P2-G6PDH WT sequence was utilised to build the putative 3D structure based on human cytosolic *Hs*G6PDH[40]. The template's quality has been predicted from features of the target-template alignment. The templates with the highest quality have then been selected for model building.

Models are built based on the target-template alignment using ProMod3.

	Template	**coverage**	**Sequence Identity**	**Sequence similarity**	**GMQE**	**QMEAN**
Monomer (*requested by user*)	5aq1.1.A	0.79	46.40	0.42	0.65	-1.73
Homo-dimer	2bh9.1A	0.79	48.31	0.43	0.66	-1.03
Homo-tetramer $NADP^+$ bound	5aq1.1.A	0.79	46.40	0.42	0.65	-1.30
Homo-tetramer $NADP^+$-G6P bound	5aq1.1.A	0.75	49. 10	0.43	0.63	-1.72

Supplemental Table S4 - Effects of heavy metals utilized in this study on G6PDH from different sources as presented in brenda database (http://www.brenda-enzymes.org/). In the third column the description of the main effects noted is provided. Where measured, changes in kinetic properties and IC_{50} values are reported in fourth column and fifth column, respectively. The original references are listed below.

Heavy metals	Organisms	Authors comments	KI	EC50	References
Lead (Pb^{++})	*Oncorhynchus mykiss*	noncompetitive inhibition	0.213 mM	0.78 mM	(2)
Nickel (Ni^{++})	*Camelus dromedarius*	95% residual activity at 2 mM			(5)
Cadmium (Cd^{++})	*Aspergilus paraticus*				(8)
	Cryptococcus neoformans				(9)
	Deinococcus radiophilus	53% of G6PDH1 inhibition at 1 mM			(10)
	Escherichia coli	83% of G6PDH inhibition at 1 mM			(1)
	Lactobacillus buchneri				(7)
	Oncorhynchus mykiss	noncompetitive inhibition	2.034 mM	1.97 mM	(2)
Copper (Cu^{++})	*Bos taurus*	65% residual activity at 2 mM (G6PD2), 50% residual activity at 2 mM (G6PD1)			(6)
	Brugia malayi				(11)
	Camelus dromedarius	15% residual activity at 5 mM			(5)
	Deinococcus radiophilus	24% inhibition of G6PDH-1 at 1 mM 78% inhibition of G6PDH-2 at 1 mM			(10)
	Escherichia coli	Complete inhibition using 1 mM of metal			(1)
	Lactobacillus buchneri				(7)
	Oncorhynchus mykiss	noncompetitive inhibition	1.721 mM	1.19 mM	(2)

Zinc (Zn^{++})	*Aspergilus aculeatus*	competitive, 40% inhibition at 0.01 mM	0.0066 mM		(4)
	Aspergilus paraticus				(8)
	Bos taurus	58% residual activity at 5 mM (G6PD2) 35% residual activity at 2 mM (G6PD1)			(6)
	Camelus dromedarius	50% residual activity at 5 mM of metal			(5)
	Cryptococcus neoformans				(9)
	Deinococcus radiophilus	83% inhibition of G6PDH-2 at 1 mM, 94% inhibition of G6PDH-1 at 1 mM			(10)
	Homo sapiens				(3)
	Lactobacillus buchneri				(7)
	Oncorhynchus mykiss	noncompetitive inhibition	2.77 mM	2.16 mM	(2)
	Sus scrofa				(3)

References to Supplemental Table S4

1. Banerjee, S. & Fraenkel, D.G. Glucose-6-phosphate dehydrogenase from Escherichia coli and from a 'high-level' mutant. *J. Bacteriol.* **110**, 155-160; (1972).
2. Cankaya, M., Sisecioglu, M., Ciftci, M. & Ozdemir, H. Effects of some metal ions on trout liver glucose 6-phosphate dehydrogenase. *Res. J. Environ. Toxicol.* **5**, 385-391 (2011).
3. Cho, S.W. & Joshi, J.G. Characterization of glucose-6-phosphate dehydrogenase isozymes from human and pig brain. *Neuroscience.* **38**, 819-828 (1990).
4. Ibraheem, O., Adewale, I.O. & Afolayan, A. Purification and properties of glucose 6-phosphate dehydrogenase from Aspergillus aculeatus. *J. Biochem. Mol. Biol.* **38**, 584-590 (2005).
5. Ibrahim, M., Ghazy, A., Salem, A., Ghazy, M. & Abdel-Monsef, M. Purification and characterization of glucose-6-phosphate dehydrogenase from camel liver. *Enzyme Res.* 2014, 714054 (2014).
6. Ibrahim, M.A., Ghazy, A.H., Salem, A.M., Ghazy, M.A. & Abdel-Monsef, M.M. Biochemical characterization of buffalo liver glucose-6-phosphate dehydrogenase isoforms. *Protein J.* **34**, 193-204 (2015).
7. Kawai, K. & Eguchi, Y. Properties of Lactobacillus glucose 6-phosphate dehydrogenase. *J. Ferment. Technol.* 57, 369-371; (1979).
8. Niehaus, W.G. & Dilts, R.P. Purification and characterization of glucose-6-phosphate dehydrogenase from Aspergillus parasiticus. *Arch. Biochem. Biophys.* **228**, 113-119; (1984).
9. Niehaus, W.G. & Mallett, T.C. Purification and characterization of glucose-6-phosphate dehydrogenase from Cryptococcus neoformans: identification as 'nothing dehydrogenase. *Arch. Biochem. Biophys.* **313**, 304-309; (1994).
10. Sung, J.Y. & Lee, Y.N. Isoforms of glucose 6-phosphate dehydrogenase in Deinococcus radiophilus. *J. Microbiol.* **45**, 318-325; (2007).
11. Verma, A., Suthar, M.K., Doharey, P.K., Gupta, S., Yadav, S., Chauhan, P.M. & Saxena, J.K. Molecular cloning and characterization of glucose-6-phosphate dehydrogenase from Brugia malayi. *Parasitology* **140**, 897-906 (2013).